Polymer Testing 76 (2019) 1–9

Contents lists available at ScienceDirect

Polymer Testing

journal homepage: www.elsevier.com/locate/polytest

Air gap membrane distillation of MEG solution using PDMS coated polysulfone hollow fiber membrane

M.A. Ajdar[a], A. Azdarpour[a,**], A. Mansourizadeh[b,*], B. Honarvar[a,c]

[a] Department of Chemical Engineering, Marvdasht Branch, Islamic Azad University, Marvdasht, Iran
[b] Department of Chemical Engineering, Gachsaran Branch, Islamic Azad University, Gachsaran, Iran
[c] Department of Civil Engineering, The University of Texas at Arlington, Arlington, TX, 76019, USA

ARTICLE INFO

Keywords:
Porous PSF hollow fiber membrane
Polydimethylsiloxane
Air gap membrane distillation
Mono-ethylene glycol

ABSTRACT

Surface modified porous polysulfone (PSF) hollow fiber membrane was prepared by dip-coating of polydimethylsiloxane (PDMS). The prepared membranes were used in an air gap membrane distillation (AGMD) process for dehydration of MEG-water mixtures. The membranes were characterized in terms of Field Emission Scanning Electronic Microscopy (FESEM), N_2 permeation, contact angle measurement and wetting pressure. From FESEM images, the prepared membrane showed a porous structure with finger-like cavities. In addition, formation of ultra-thin coating layer on the inner and outer surface was confirmed by FESEM. From N_2 permeation test, the modified membrane showed smaller mean pore size (9 nm) and lower surface porosity compared to the plain membrane. The modified membrane showed a good hydrophobicity with water contact angle of 118° and wetting pressure of 800 kPa. The permeate flux of about 26 kg/m^{2}h was obtained for the modified membrane at MEG concentration of 20 wt%, feed temperature of 90 °C and feed velocity of 0.66 m/s. Due to the improved structure, the modified membrane showed a stable AGMD operation for 80 h compared to the plain membrane.

1. Introduction

Mono-ethylene glycol (MEG) is one of the most favored hydrate inhibitors used in hydrocarbon transportation pipelines and processing facilities. It has several properties such as low volatility, low toxicity, low flammability, favorable thermodynamic behavior, simple and proven technology requirements and high availability [1]. In economic point of view, it usually essential to separate MEG from the produced water, so that it can be recovered to reduce the operating costs. The regeneration process, with high energy consumption, is the basic MEG recovery method and is comprised of a simple distillation column to remove most of the water [2]. Therefore, cost effective separation technologies are required in the chemical industries in order to be economical. Membrane distillation (MD) which involves membrane and distillation systems can be a good alternative to the traditional distillation processes. So far, MD has been used in several separation processes, such as desalination [3–5], wastewater treatment [6–9], and food industries [10,11]. MD is a non-isothermal membrane process which has been introduced for about fifty years, however there is still need to be improved for sufficient industrial application [12]. In MD, vapor pressure gradient across a porous hydrophobic membrane results in transportation of vapor molecules from high vapor pressure to the low vapor pressure. In general, four main configurations are known for MD which are air gap (AGMD), sweeping gas (SGMD), vacuum (VMD) and direct contact (DCMD) [13–15].

MD can be an alternative for concentrating aqueous solutions of dihydric alcohol or poly-alcohols such as MEG, diethylene glycol (DEG) and glycerol, which are usually non-volatile or semi-volatile. Porous polytetrafluoroethylene (PTFE) membranes for dehydration of DEG by a VMD process was studied by Chen and Huang [16]. The results showed that the water content in the feed solution was reduced from 15 wt% to 2 wt% in 100 min. VMD at the condition of 90 °C, stirring speed of 1500 rpm and vacuum of 715 torr. Continuous-effect membrane distillation (CEMD) process was applied to concentrate aqueous glycerol solution by using a hollow fiber AGMD module [17]. From the experiments it was found that a feed of 10 g/L could be concentrated up to about 400 g/L with a rejection efficiency of more than 99.9%. In another study, commercial PTFE membranes were applied for DCMD of water-ethylene glycol mixtures [18]. The experiments showed complete rejection of glycol where an effective concentration was achieved.

* Corresponding author.
** Corresponding author.
E-mail addresses: amin.azhdarpour@miau.ac.ir (A. Azdarpour), a.mansourizadeh@yahoo.com (A. Mansourizadeh).

https://doi.org/10.1016/j.polymertesting.2019.03.002
Received 11 November 2018; Received in revised form 26 February 2019; Accepted 1 March 2019
Available online 06 March 2019
0142-9418/ © 2019 Elsevier Ltd. All rights reserved.

Mohammadi and Akbarabadi [19] investigated VMD of MEG-water mixtures at different temperature and circulation rates by using a flat-sheet polypropylene membrane module. The results showed that by increasing temperature and recirculation rate the permeate flux was increased with no effect on MEG rejection. Moreover, increasing of feed flow rate higher than 0.67 L/min had no significant effect on the permeate flux. Shirazi et al. [6] studied SGMD of dilute glycerol wastewater using a flat-sheet PTFE membrane module. The effects of operating parameters such as feed temperature, feed flow rate, sweep gas flow rate and glycerol concentration in aqueous phase on the permeate flux were investigated. The maximum permeate flux of about 21 L/m^2 h was achieved at the optimum conditions.

Comparing with the other MD configurations, AGMD has several advantages such as no contact of permeate with membrane, relatively high flux, low heat lost and less fouling tendency [20]. In AGMD, the membrane module holds a stagnant air gap between the membrane and a condensation surface which is placed inside the module. The temperature difference between the feed solution and the cold surface is the driving force for evaporation of volatile compounds at the hot liquid-vapor interfaces which is formed at the mouth of the membrane pores. It should be noted that research on AGMD of glycol solutions are limited in the literature.

The membrane properties such as surface porosity (permeability) and hydrophobicity are important parameters in order to achieve a worthy permeate flux in a MD process. Polysulfone (PSF) has been applied for preparation of the membranes due to good mechanical strength, thermal and chemical stability. Therefore, this study aims to prepare a highly porous PSF hollow fiber membrane by a phase-inversion process. Phase-inversion behavior of the polymer solution was evaluated through the cloud point measurements in order to achieve a solution composition for improving the membrane surface porosity. A dip-coating process by polydimethylsiloxane (PDMS) was conducted in order to enhance surface hydrophobicity of the membrane with a minimum influence on the surface porosity. The plain and modified membrane modules were prepared and used in the AGMD process for dehydration of MEG-water mixtures. The prepared membranes were characterized in terms of Field Emission Scanning Electronic Microscopy (FESEM), gas permeation, contact angle measurement and wetting pressure. The effect of feed temperature, feed flowrate and MEG concentration in the liquid phase on the permeation flux of the membrane was investigated through the AGMD system. In addition, long-term stability of the membranes was studied for the AGMD operation.

2. Experimental

2.1. Materials

Polysulfone (Udel P-1700) in pellet form (Solvay Advance Polymers) was used for the fabrication of hollow fiber membranes. 1-methyl-2-pyrrolidone (NMP, > 99.5%) was provided by MERCK and used as the polymer solvent. Glycerol was purchased from MERCK and used as the non-solvent additive in the polymer solution. The polydimethylsiloxane (PDMS) (Sylgard 184, Dow Corning) was prepared using 10:1 mixture of the base polymer and the curing agent where n-hexane was used as the solvent for PDMS. The PDMS solution of 0.5 wt % was used for surface coating of the hollow fiber membranes. Ethanol was purchased from Sigma-Aldrich and used for post-treatment of the membranes. MEG anhydrous 99.8% (Sigma-Aldrich) was used to prepare the feed solutions for AGMD experiments.

2.2. Cloud point measurements

In order to study phase-inversion of the polymer solution, cloud point diagram of PSF/NMP/glycerol/water was measured using a titration method. To measure the cloud points, the polymer solutions were prepared at constant 6 wt% glycerol in NMP and the polymer concentration in the range of 1–20 wt%. The cloud points were obtained at 25 °C by addition of distilled water droplets using a burette under a constant stirring. When a local precipitation occurred at the high polymer concentration, the stirring was continued to achieve a homogeneous solution. More water droplets were added into the solution to achieve a cloudy form. Composition of the solution at the cloud point was measured by weight.

Table 1
Spinning conditions for hollow fiber membrane fabrication.

Parameter	value
Dope Extrusion Velocity (cm/s)	8.5
Bore Fluid Velocity (cm/s)	25.5
Bore Composition (wt.%)	NMP/H_2O 70/30
External Coagulant	Tap Water
Air Gap Distance (cm)	0.0
Spinneret o.d/i.d. (mm/mm)	0.7/0.3
Spinning Dope Temperature (°C)	25
External Coagulant Temperature (°C)	25
Jet-Stretch Ratio[a]	1

[a] The ratio of wind up drum velocity to the dope extrusion velocity.

2.3. Fabrication of PSF hollow fiber membranes

The PSF pellets were dried at 60 ± 2 °C in a vacuum oven for 24 h to remove the moisture content. Using 17 wt% PSF, 4 wt% glycerol and 79 wt% NMP, the homogeneous polymer solution was prepared under stirring at 60 °C. The prepared solution was de-bubbled under 15 min sonication and kept for 24 h at room temperature before spinning. The hollow fiber membranes were fabricated by a wet spinning process. Table 1 exhibits the detailed spinning conditions. The fresh hollow fibers were immersed in distilled water for 3 days to remove the residual solvent and non-solvent. Post treatment of the fibers was conducted by immersion in pure ethanol for 15 min in order to minimize fiber shrinkage and pore collapse before drying at room temperature.

2.4. Surface modification of PSF hollow fiber membranes

In order to enhance surface hydrophobicity of porous PSF hollow fiber membranes, a dip-coating method by 0.5 wt% solution of PDMS was conducted. PDMS is known as one of the intrinsically hydrophobic materials which has water contact angle of about 115° [21]. In this study, the prepared porous PSF hollow fiber membranes were immersed in the PDMS solution for 2 h under constant stirring. Then the hollow fibers were kept in a vacuum oven for 12 h at 70 °C to remove n-hexane. The modified membranes were subjected to the characterization experiments.

2.5. Characterization of PSF hollow fiber membranes

2.5.1. Field emission scanning electronic microscopy (FESEM)

Structural morphology of the prepared PSF hollow fiber membranes was evaluated via a field emission scanning electronic microscopy (Hitachi S-4700 FE-SEM). To prepare the membrane samples, the dried fibers were immersed in liquid nitrogen and fractured carefully. Before capture images of the fibers, they were coated by sputtering platinum. The FESEM micrographs of cross-section, outer skin layer, inner surface and outer surface of the hollow fibers were taken at various magnifications.

2.5.2. Gas permeation test

Gas permeation test using an inert gas such as N_2 has been employed to estimate mean pore size and effective surface porosity of porous membranes [22–24]. In the present study, the testing apparatus

was based on the constant pressure method. The membrane module containing two hollow fibers with the length of about 10 cm was applied to measure N_2 permeance. Pure N_2 was supplied to the shell side of the module and the permeation flowrate was measured from the lumen side at room temperature by a soap bubble flow meter. The upstream pressure was increased from 100 kPa to 200 kPa at intervals of 20 kPa. The N_2 permeance was calculated according to the outer surface of the hollow fibers. Assuming cylindrical pores on the outer skin layer of the membrane, the overall N_2 permeance through the membrane can be expected as summation of Poiseuille and Knudsen flows [25]:

$$J_A = \frac{2rp\varepsilon}{3RTL_p}\left(\left(\frac{8RT}{\pi M}\right)^{0.5}\right) + \frac{r_p^2}{8\mu RT}\frac{\varepsilon}{L_p}\bar{P} \quad \text{or} \quad JA = K_0 + P_0\bar{P} \tag{1}$$

Where J_A is the N_2 permeance (mol/m^2 s Pa); r_p and Lp are pore radius and effective pore length, respectively (m); ε is surface porosity which is defined as ratio of the area of pores over total surface area of the fiber; R is gas constant 8.314 (J/mol K); μ is N_2 viscosity (Kg/m s); M is N_2 molecular weight (kg/mol); T is gas temperature (K); and $\bar{P}$ is mean pressure (Pa). By plotting J_A vs. mean pressures according to Eq. (1) and obtaining the intercept (K_0) and slope (P_0), mean pore size and effective surface porosity over pore length can be estimated as:

$$r_p = 5.33\left(\frac{P_0}{K_0}\right)\left(\frac{8RT}{\pi\mu}\right)^{0.5}\mu \tag{2}$$

$$\frac{\varepsilon}{Lp} = \frac{8\mu RTP0}{r_p^2} \tag{3}$$

2.5.3. Contact angle measurement

In order to measure water contact angle (CA), the membrane sample was dried in a vacuum oven at 60 °C for 12 h. The Force Tensiometer (KRÜSS) equipment was used to measure outer surface contact angle of the hollow fiber membranes. By setting water droplet size of 0.2 μl and drop rate of 0.5 μL/s, the mean values of contact angle for left and right sides of any droplets were obtained. The CA values of each sample were obtained at ten various position of the sample and then averaged. In addition, the variation of CA as a function of time for each membrane was evaluated.

2.5.4. Wetting pressure

Wetting pressure test were conducted to estimate the wetting resistance of the prepared porous membranes. In this test, by using a diaphragm pump, distilled water was pressurized in the lumen side of the hollow fibers with dead-ends. The pressure was slowly increased at 0.5 bar intervals and the fibers were kept at any constant pressure for 30 min to check if any water droplet appeared in the outer surface. The pressure for appearance of first droplet on the outer surface of the membrane was considered as wetting pressure.

2.5.5. Air gap membrane distillation experiment

For membrane distillation test, the stainless steel MD module was prepared by random packing of 20 hollow fibers with effective length of 15 cm. The approximate distance between the distributed fibers in the module was 2 mm and the air gap width was about 4 mm. The configuration of the module is shown in Fig. 1. The characteristics of the membrane module are given in Table 2. Then, the prepared module was placed in the AGMD system as shown in Fig. 2.

The MEG solutions of 20–80 wt% was flowed by a diaphragm pump through the lumen side of hollow fibers. Temperature of the MEG solution was controlled in the range of 60–90 °C by an electric heater in the solution tank. The liquid phase velocity in the lumen side of the fibers was set 0.66 m/s and the gage pressure was adjusted to 50 kPa. The shell side temperature of the membrane module was set to 10 °C using a coolant heat exchanger. The pure water flux was calculated as below:

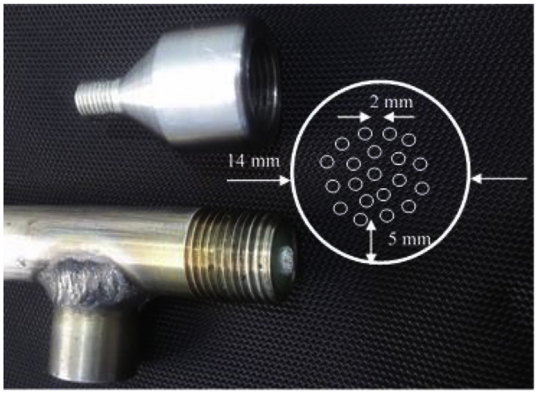

Fig. 1. Configuration of the air gap membrane distillation module.

Table 2
Characteristics of the membrane distillation module.

Parameter	Value
Module o.d. (mm)	14
Module length (mm)	250
Effective fibers length (mm)	150
Fiber o.d. (mm)	0.67
Fiber i.d. (mm)	0.35
Number of fibers	20
Membrane area (m^2)	0.0066

$$J_w = \frac{m}{A_i \times t} \tag{4}$$

Where m (kg) represents the weight of produced water in time t (h), and A_i (m^2) is the inner surface of the hollow fibers in the membrane module.

3. Results and discussion

3.1. Cloud points of the PSF solutions

Coagulation rate of the polymer solution plays an important role on the properties of the prepared membrane where a fast coagulation can result in porous and anisotropic membranes [26]. Introducing a non-solvent additive into the polymer solution can cause an instable thermodynamic condition and increase the coagulation rate of the polymer solution [27]. In the present study, glycerol as a strong non-solvent additive was added into the PSF solution to improve phase-inversion rate and prepare porous membranes. Phase-inversion behavior of the PSF solutions was quantitatively studied by cloud point measurements and the ternary phase diagram is shown in Fig. 3. As can be seen, by addition of glycerol, the isothermal cloud points moved toward the polymer–solvent axis which reveals that less water is required for coagulation of the solutions. A similar trend was observed by addition of different types of additives in the PSF solution [23]. From Fig. 3, for PSF solution of 17 wt%, about 5.5 wt% and 1 wt% water was required for coagulation of the plain solution and the solution with 6% glycerol, respectively. Since the PSF solution with 6% glycerol was close to the coagulation state, it could result in a dense and sponge-like structure. Liu et al. [28] prepared the polyethersulfone solutions close to the coagulation state which resulted in hollow fiber membranes with sponge-like and macrovoid free structure. Indeed, the sponge-like structure can provide a high degree of tortuosity which can affect the permeate flux of MD [29]. Therefore, in the present study, in order to prepare a membrane with an open structure, 4 wt% of glycerol was used in the PSF solution of 17 wt%. About 1.5 wt% water was required

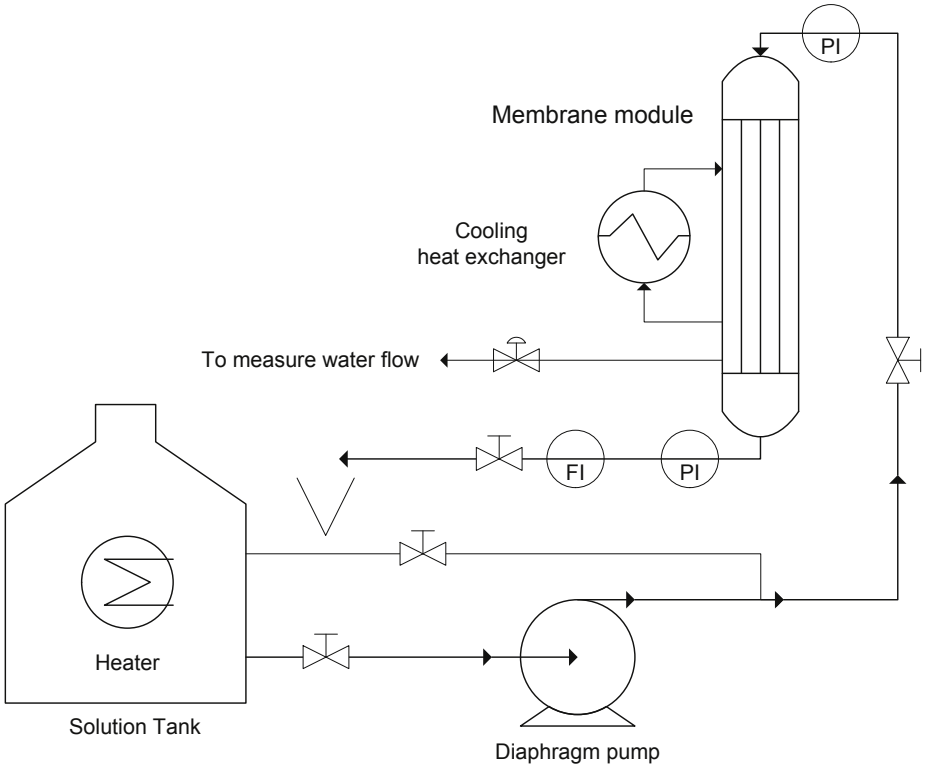

Fig. 2. Schematic of the air gap membrane distillation system.

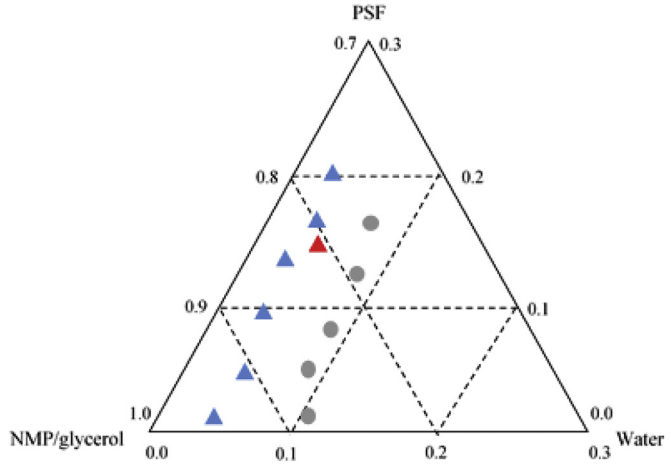

Fig. 3. Cloud point diagram of PSF/NMP/glycerol/water system at 25 °C: ● plain solutions; ▲solutions with 6% glycerol; and ▲ spinning solution with 4% glycerol.

for coagulation of the prepared solution which confirmed an instable thermodynamic state. This solution is expected to generate an open membrane structure with large finger-like macrovoids which can result in high permeate flux for the MD application.

3.2. Morphology of the prepared hollow fiber membranes

FESEM micrographs of cross-section, outer skin layer, inner skin layer, inner surface and outer surface were obtained to evaluate morphology of the prepared PSF hollow fiber membranes. The membranes possess an average inner diameter of 350 μm and outer diameter of 670 μm. FESEM micrographs of the plain membrane are shown in Fig. 4. The plain PSF membrane showed large finger-likes, which extended from the outer surface to near the inner layer of the membrane. The addition of glycerol into the spinning solution can cause thermodynamic instability, which improved liquid–liquid phase separation. This phenomenon resulted in generation of large finger-likes and a thin outer skin. It should be noted that thermodynamic and kinetic effects of the polymer solution during phase separation controls the final membrane structure. In general, the addition of non-solvent additives in the polymer solution results in improvement of phase separation, which produces membranes with open structure (thermodynamic effect). In contrast, the addition of non-solvent additives can increase the solution viscosity, which results in reduction of solvent/non-solvent exchange rate during the phase separation process and produces a denser membrane structure (kinetic effect). Type and concentration of non-solvent additives can affect thermodynamic and kinetic, which is useful for tailoring the membrane properties such as permeation flux, separation factor and morphology [30]. In this case, due to the low viscosity of the PSF solution containing 4 wt% glycerol (870 cp at 25 °C), it seems that the kinetic effect was not important and the thermodynamic effect controlled the membrane structure.

As shown in Fig. 4 (3,4), a delay phase separation from the bore side produced a sponge-like sublayer which can be related to the use of 70% NMP solution as the bore fluid. In fact, using a weak non-solvent in the bore side results in reducing the polymer concentration and the delay solidification of the localized polymer-rich phase could generate an open-cell structure. The prepared membrane illustrated an inner skinless layer. A similar morphology was reported for the PSF hollow fiber membrane when using different NMP aqueous solutions as the bore fluid [31].

Fig. 5 shows FESEM micrographs of the modified PSF hollow fiber membrane. As can be seen, there was no significant changes in cross-sectional morphology. However, an ultra-thin coated layer with thickness of about 100 nm was formed on the outer surface of the membrane.

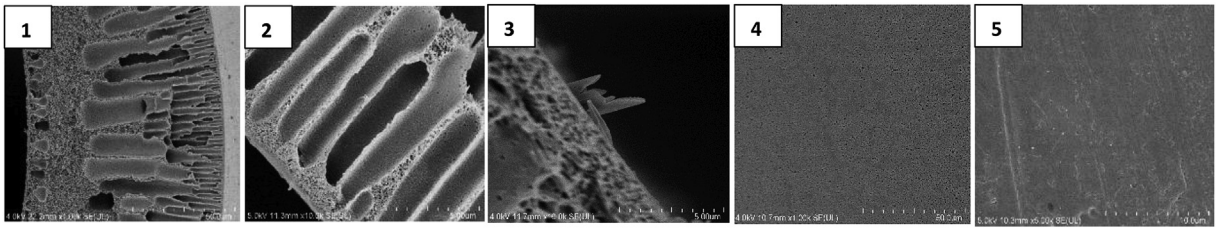

Fig. 4. FESEM micrographs of the plain PSF hollow fiber membrane, (1) cross section; (2) outer skin layer; (3) inner skin layer; (4) inner surface; and (5) outer surface.

In addition, it seems that a thin layer of PDMS was also formed on the inner surface of the membrane. Li et al. [32] studied the details of PDMS casting on the surface of the ultrafiltration flat PSF membrane. It was found that by increasing the casting thickness from 100 to 500 μm the N_2 permeance of the composite membrane reduced from 259 to 128 GPU, respectively. This significant N_2 permeance reduction was related to the higher thickness and penetration of PDMS to the PSF layer. In the present study, due to the formation of ultra-thin coated layer a good gas permeability can be expected for the prepared composite PSF-PDMS hollow fiber membrane. In fact, highly permeable hydrophobic membranes with good surface porosity can enhance water flux of the MD process.

3.3. Properties of PSF hollow fiber membranes

The main objective of this study was to enhance surface hydrophobicity of the PSF hollow fiber membrane without a significant reduction in the gas permeability. For this purpose, an ultra-thin layer of PDMS was coated on the surface of the membrane. The structure of the prepared membranes was characterized in terms of N_2 permeability, wetting pressure and water contact angle. The characterization results are given in Table 3.

Mean pore size and effective surface porosity of the membranes were measured by N_2 permeation test and the results are given in Table 3. N_2 permeance as function of mean pressure for the membranes was plotted in Fig. 6. The values of slope (P_0) and intercept (K_0) of the solid lines (the best linear fit to the data) were obtained to estimate the mean pore size and the effective surface porosity by Eqs. (2) and (3). Since the slope of N_2 permeance line for the PSF membranes is reasonably low, it shows that Poiseuille flow controls permeability through the membrane pores. This confirms nano-scale pore sizes of the membrane, as shown in Table 3. The modified PSF membrane illustrated N_2 permeance of 820 GPU at 100 kPa which is significantly lower than N_2 permeance of the plain membrane. Although an ultra-thin PDMS coating layer was formed on the membrane surface, the intrusion of PDMS into the pores could result in pore size and surface porosity reduction. Due to the low viscosity of the PDMS solution (0.5 wt%), it is subjected to penetrate the membrane pores. In a similar study for composite flat PSF membranes, by increasing PDMS casting thickness a significant N_2 permeance reduction was observed for the prepared composite membrane [32].

Wetting pressure and contact angle measurement were conducted to evaluate wetting resistance of the PSF hollow fiber membranes. The measured outer and inner surfaces contact angle values of the PSF hollow fiber membranes are given in Table 3. As can be seen, PDMS modification resulted in enhancement of the outer surface contact angle from about 83° to 118° and the inner surface from about 77° to 97°. This significant hydrophobicity improvement can confirm a good PDMS coating process. Indeed, membrane hydrophobicity is the main factor in a MD process which can significantly affect the produced flux. In the present study, since the MEG solution is flowed in the lumen side of the hollow fiber membranes in the module, the improvement of the inner surface hydrophobicity can minimize the membrane wetting during the AGMD process. Measured contact angle of the membranes as function of the contact time with water is shown in Fig. 7. After 60 s, the plain membrane showed about 6% reduction in the inner and outer surfaces contact angle which confirms wetting tendency of the membrane. On the other hand, the PDMS coated membrane showed about 1.5–2% reduction in the inner and outer surfaces contact angle which demonstrated higher wetting stability of the membrane for the MD process. The prepared PSF membranes stability in the AGMD process will be discussed in the later section.

For wetting pressure, as stated by Laplace–Young equation (Eq. (5)), the pressure difference that is required for penetration of the liquid in the membrane pores is proportional to pore size, surface contact angle and surface tension of the liquid [33].

$$\Delta P = -\frac{2\gamma\ cos\theta}{r_{p,m}} \tag{5}$$

Where γ is surface tension of the liquid phase (N/m); θ is the contact angle between the membrane surface and the liquid; and $r_{p,m}$ is maximum pore size of the membrane (m).

From Table 3 can be seen that the plain PSF membrane has a relatively lower wetting pressure compared to the modified PSF membrane. Since the PDMS coated membrane showed smaller mean pore size and higher surface hydrophobicity, the high wetting pressure of about 800 kPa can be confirmed. Therefore, the combined effects of smaller pore size and higher hydrophobicity decreased the possibility of the membrane wetting. It should be noted that the modified membrane can easily withstand wetting for the membrane distillation process which is operated at a low pressure difference of 50 kPa (in this case).

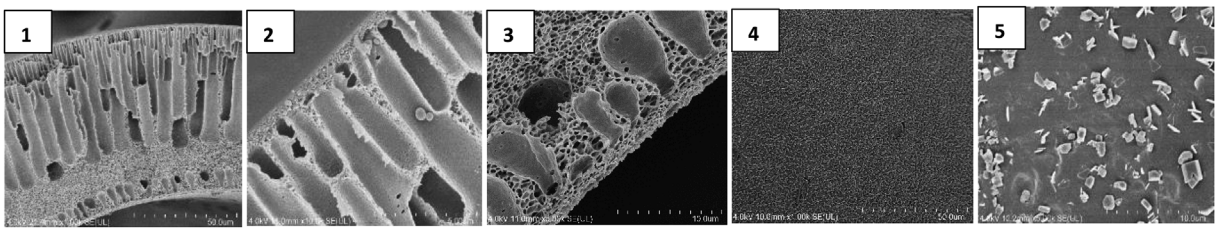

Fig. 5. FESEM micrographs of modified PSF hollow fiber membrane, (1) cross section; (2) outer skin layer; (3) inner skin layer; (4) inner surface; and (5) outer surface.

Table 3
Properties of PSF hollow fiber membranes.

Membrane	N_2 permeance @100 kPa (GPU)	Mean pore size (nm)	Surface porosity (m^{-1})	Wetting pressure (kPa)	Outer surface contact angle (°)	Inner surface contact angle (°)
Plain PSF	4050	18	872	500	82.8 ± 1.38	76.5 ± 1.31
Modified PSF	820	9	35	800	118 ± 0.63	98.2 ± 0.41

3.4. AGMD performance of the PSF hollow fiber membranes

Fig. 8 shows water flux of the prepared membranes as function of the feed temperature at constant MEG concentration of 20 wt% and the feed velocity of 0.66 m/s. The experiments were conducted at the feed temperature in the range of 60–90 °C, while the coolant surface temperature was kept constant at 10 °C. A significant improvement was observed in the water flux of the membranes by increasing temperature. Since the driving force of mass transfer for MD processes is vapor pressure difference across the membrane, increasing temperature can increase vapor pressure based on Antoine equation and subsequence flux improvement. In addition, increasing temperature can increase water vapor diffusion coefficient through the membrane pores which results in improvement of the flux [34]. From Fig. 8, the modified PSF membrane showed a relatively smaller water flux compared to the plain membrane. As mentioned earlier, the modified membrane with smaller pore size and surface porosity provided a smaller contact area which can result in a lower water flux. At 90 °C the modified membrane showed water flux of about 26 kg/m^2 h which is 13% less than the flux of the plain membrane. However, due to the enhanced surface hydrophobicity of the modified membrane, a more stable AGMD operation can be expected.

For the modified membrane, the effect of operating parameters such as MEG concentration and the feed velocity on the permeate flux is shown in Fig. 9. For the effect of feed velocity, at the constant feed temperature of 90 °C and MEG concentration of 20%, it can be seen that a slight improvement in the water permeate flux was observed when the velocity increased from 0.33 to 1.32 m/s. However, a severe reduction in water permeate flux was observed by increasing MEG concentration in the feed solution from 20 to 80 wt% at the constant feed velocity of 0.66 m/s and feed temperature of 90 °C. In fact, by increasing the feed velocity, reduction of temperature and concentration boundary layer thickness can result in a decrease in the mass and heat transfer resistance [35,36]. This phenomena could reduce temperature and concentration difference between the bulk liquid and the membrane surface which improved permeate flux of the membrane, consequently. From Fig. 9, this effect is more sever at a higher feed velocity, since an insignificant effect on the flux was observed at the velocity higher than 0.99 m/s. As for MEG concentration in the feed, an increase in the concentration results in reduction of vapor pressure and water activity which plays an important role in the permeate flux reduction [36]. In fact, reduction of vapor pressure can minimize vaporization of at the membrane surface resulting in a decline of vapor diffusion through the membrane pores. Mohammadi and Akbarabadi [19] reported that about 53% flux reduction was attained in a VMD process when MEG concentration increased from 20 to 60% at the feed flowrate of 0.8 L/min and the temperature of 60 °C.

In order to evaluate stability of the prepared PSF hollow fiber membranes, a long-term AGMD operation for about 80 h was conducted and the results are given in Fig. 10. The test was performed at constant the feed velocity of 0.33 m/s, the temperature of 90 °C and MEG concentration of 20 wt%. As can be seen for the plain PSF membrane, the sharp decline of the permeate flux during initial 6 h of the operation can be related to the partial wetting. Although the plain membrane showed higher permeate flux at initial stage of the operation due to the higher surface porosity, the severe flux reduction can be attributed to the lower surface hydrophobicity and the larger pore size. The permeate flux of the plain membrane was reduced from 25 kg/m^2h to about 13 kg/m^2h during 80 h of the operation. On the other hand, the modified PSF membrane with higher surface hydrophobicity and wetting resistance showed a more stable AGMD operation. A gradual flux reduction of about 27% was observed during 80 h of the operation.

Dehydration performance of poly-alcohols by different MD processes was compared in Table 4. Hydrophobic commercial polypropylene (PP) and PTFE membranes have been used in different MD processes. As can be seen, the permeate flux of the commercial

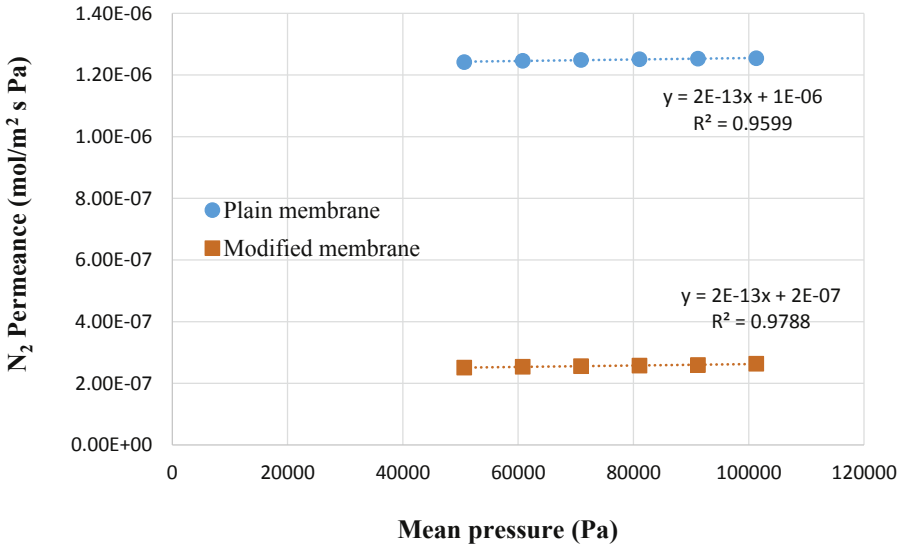

Fig. 6. N_2 permeance of the PSF hollow fiber membranes as function of mean pressure.

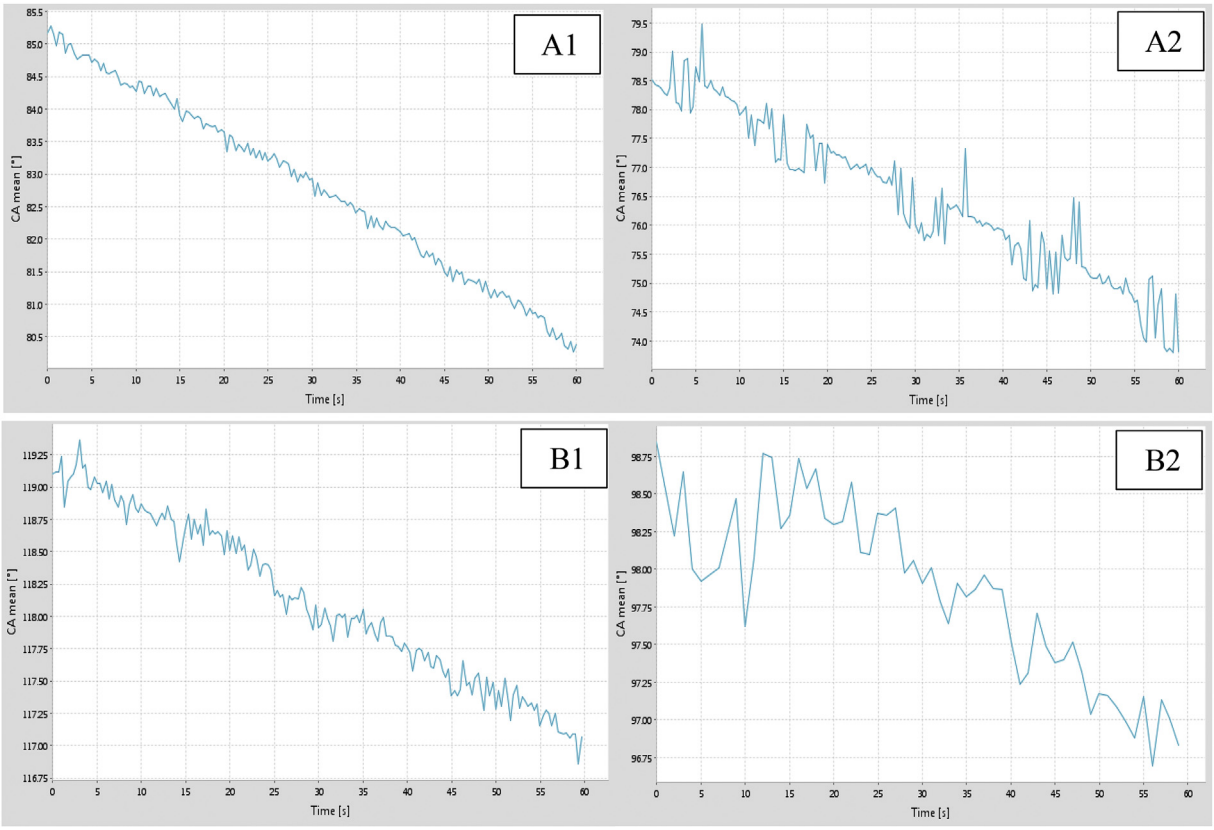

Fig. 7. Water contact angle of the PSF hollow fiber membranes as function of contact time: (A) Plain PSF; (B) Modified PSF; (1) Outer surface; and (2) Inner surface.

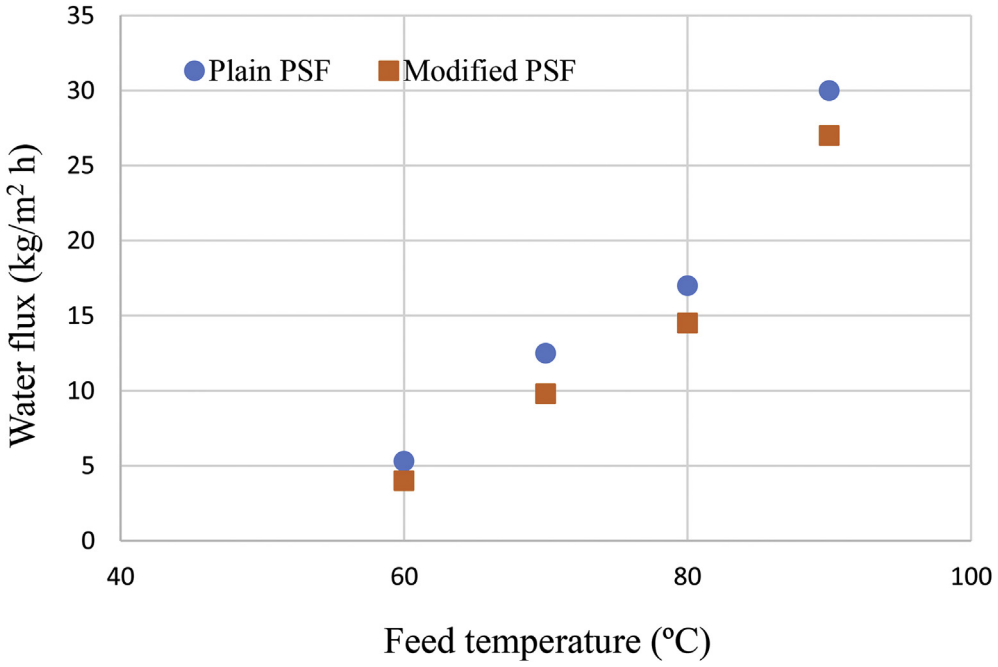

Fig. 8. Effect of temperature on water flux of the PSF hollow fiber membranes (V_F = 0.66 m/s and C_{MEG} = 20 wt%).

membranes is relatively lower than the flux of the in-house made asymmetric PSF membrane. It should be noted that commercial PP and PTFE membranes are usually prepared by stretching and thermal methods [37,38], which demonstrate large pore size and low surface porosity. The modified PSF membrane prepared in the present work has good hydrophobicity, high wetting resistance and surface porosity which resulted in a reasonable permeate flux.

4. Conclusion

In the present study, porous PSF hollow fiber membrane was prepared by a phase-inversion process. Modification by PDMS coating was conducted to enhance surface hydrophobicity of the membrane. The structure of the membranes was characterized in terms of FESEM, N_2 permeation, water contact angle and wetting pressure. The plain and

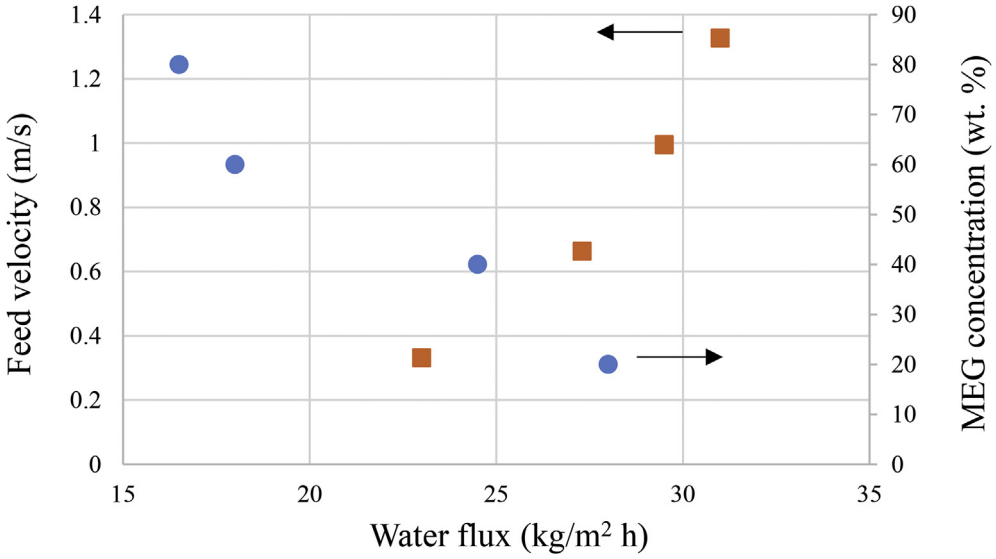

Fig. 9. Effect of feed velocity and MEG concentration on the water flux of the modified PSF hollow fiber membrane.

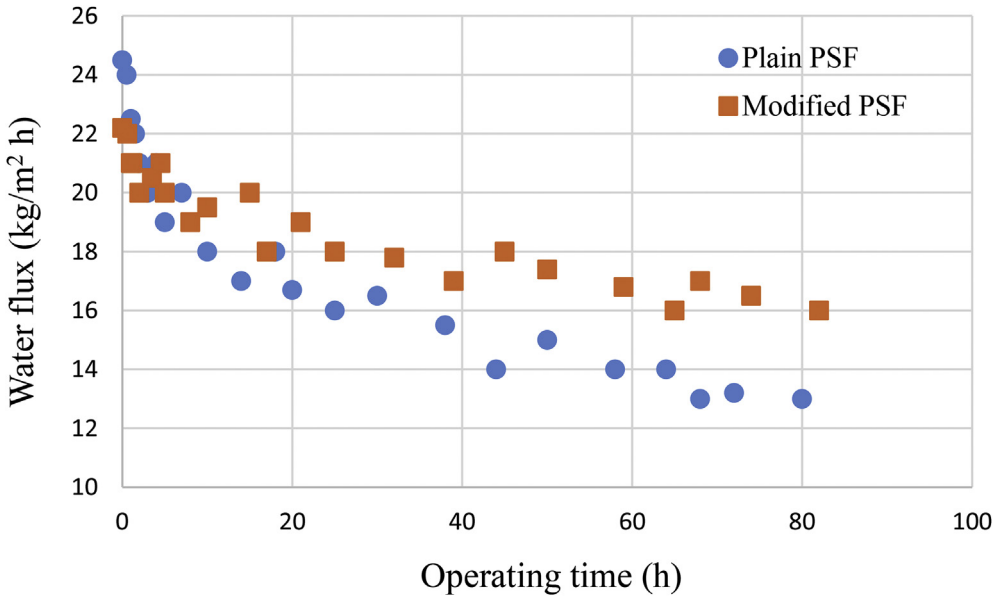

Fig. 10. Water flux of the PSF membranes as function of operating time in long-term AGMD experiments (CMEG = 20 wt%; V_F = 0.33 m/s; and TF = 90 °C).

Table 4
Comparison of different MD processes for dehydration of poly-alcohols.

Membrane	Pore size (μm)	Distillation process	Remarks	Permeate flux (kg/m^{2}h)	Ref.
Commercial PP	0.2	VMD	MEG solution 60 wt%, T_h = 60 °C, Q_f = 0.8 L/min	6	[19]
Commercial PP	0.2	AGMD	Glycerol solution 20 wt%, T_h = 90 °C, T_c = 30 °C, Q_f = 30 L/h	5.5	[17]
Commercial PTFE	0.2	VMD	DEG solution 85 wt%, T_h = 90 °C, vacuum degree = 715 torr	17.32	[16]
Commercial PTFE	0.2	DCMD	MEG solution 37 wt%, T_h = 65 °C, T_c = 25 °C	20	[18]
Commercial PTFE	0.22	SGMD	Glycerol solution 5 wt%, T_h = 65 °C	13.54	[6]
Modified PSF present work	0.009	AGMD	MEG solution 20 wt%, T_h = 90 °C, T_c = 10 °C, Q_f = 100 ml/min	26	–

modified membrane modules were prepared and used in the AGMD process for dehydration of the MEG solutions. The main findings can be summarized as follows:

- From N_2 permeation test, the modified membrane showed smaller mean pore size (9 nm) and lower surface porosity compared to the plain membrane.
- The modified membrane showed a good hydrophobicity with water contact angle of 118°.
- Modification by PDMS resulted in improvement of wetting pressure of the membrane from 500 to 800 kPa.
- The modified membrane illustrated permeate flux of about 26 kg/m^{2}h at MEG concentration of 20 wt%, feed temperature of 90 °C and feed velocity of 0.66 ml/min.
- A more stable AGMD operation was observed for the modified membrane compared to the plain membrane. The modified

membrane showed a gradual flux reduction of about 27% during 80 h of the operation.

- In comparison with the commercial PP and PTFE membrane, a reasonable permeate flux was obtained for the modified PSF membrane due to the improved structure.

Acknowledgment

The authors gratefully acknowledge the financial support of Islamic Azad University, Marvdasht, Iran.

References

[1] A. Yong, E.O. Obanijesu, Influence of natural gas production chemicals on scale production in MEG regeneration systems, Chem. Eng. Sci. 30 (2015) 172–182.
[2] M.N. Psarrou, L.O. Josang, K. Sandengen, T. Ostvold, Carbon Dioxide solubility and Monoethylene Glycol (MEG) degradation at MEG reclaiming/regeneration conditions, J. Chem. Eng. Data 56 (2011) 4720–4724.
[3] D.L.M. Mendez, C. Castel, C. Lemaitre, E. Favre, Membrane distillation (MD) processes for water desalination applications. Can dense selfstanding membranes compete with microporous hydrophobic materials? Chem. Eng. Sci. 188 (2018) 84–96.
[4] A. Hagedorn, G. Fieg, D. Winter, J. Koschikowski, T. Mann, Methodical design and operation of membrane distillation plants for desalination, Chem. Eng. Res. Des. 125 (2017) 265–281.
[5] A. Rastegarpanah, H.R. Mortaheb, Surface treatment of polyethersulfone membranes for applying in desalination by direct contact membrane distillation, Desalination 377 (2016) 99–107.
[6] M.M.A. Shirazi, A. Kargari, M. Tabatabaei, A.F. Ismail, T. Matsuura, Concentration of glycerol from dilute glycerol wastewater using sweeping gas membrane distillation, Chem. Eng. Process. Process Intensif. 78 (2014) 58–66.
[7] M. Madhumala, D. Madhavi, T. Sankarshana, S. Sridhar, Recovery of hydrochloric acid and glycerol from aqueous solutions in chloralkali and chemical process industries by membrane distillation technique, J. Taiwan Inst. Chem. Eng. 45 (2014) 1249–1259.
[8] P.M. Duyen, P. Jacob, R. Rattanaoudom, C. Visvanathan, Feasibility of sweeping gas membrane distillation on concentrating triethylene glycol from waste streams, Chem. Eng. Process. Process Intensif. 110 (2016) 225–234.
[9] R. Moradi, J. Karimi-Sabet, M. Shariaty-Niassar, Y. Amini, Air gap membrane distillation for enrichment of H2 18O isotopomers in natural water using poly(vinylidene fluoride) nanofibrous membrane, Chem. Eng. Process. Process Intensif. 100 (2016) 26–36.
[10] M. Gryta, M. Tomaszewska, J. Grzechulska, A.W. Morawski, Membrane distillation of NaCl solution containing natural organic matter, J. Membr. Sci. 181 (2001) 279–287.
[11] K.V. Kotsanopoulos, I.S. Arvanitoyannis, Membrane processing technology in the food industry: food processing, wastewater treatment, and effects on physical, microbiological, organoleptic, and nutritional properties of foods, Crit. Rev. Food Sci. Nutr. 55 (2015) 1147–1175.
[12] M. Khayet, Membranes and theoretical modeling of membrane distillation: a review, Adv. Colloid Interface Sci. 164 (1–2) (2011) 56–88.
[13] M. Khayet, T. Matsuura, Membrane Distillation Principles and Applications, Elsevier, Oxford, UK, 2011.
[14] M.S. El-Bourawi, Z. Ding, M. Khayet, Review a framework for better understanding membrane distillation separation process, J. Membr. Sci. 285 (2006) 4–29.
[15] P. Wang, T.S. Chung, Recent advances in membrane distillation processes: membrane development, configuration design and application exploring, J. Membr. Sci. 474 (2015) 39–56.
[16] T.-H. Chen, Y.-H. Huang, Dehydration of diethylene glycol using a vacuum membrane distillation process, J. Taiwan Inst. Chem. Eng. 74 (2017) 233–237.
[17] K. Zhang, Y. Qin, F. He, J. Liu, Y. Zhang, L. Liu, Concentration of aqueous glycerol solution by using continuous-effect membrane distillation, Separ. Purif. Technol. 144 (2015) 186–196.
[18] C. RincoÂn, J.M.O. de Zarate, J.I. Mengual, Separation of water and glycols by direct contact membrane distillation, J. Membr. Sci. 158 (1999) 155–165.
[19] T. Mohammadi, M. Akbarabadi, Separation of ethylene glycol solution by vacuum membrane distillation (VMD), Desalination 181 (2005) 35–41.
[20] E. Drioli, A. Ali, F. Macedonio, Membrane distillation: recent developments and perspectives, Desalination 356 (2015) 56–84.
[21] X. Li, B. Chen, W. Cai, T. Wang, Z. Wu, J. Li, Highly stable PDMS–PTFPMS/PVDF OSN membranes for hexane recovery during vegetable oil production, RSC Adv. 7 (2017) 11381–11388.
[22] R. Naim, A.F. Ismail, A. Mansourizadeh, Preparation of microporous PVDF hollow fiber membrane contactors for CO_2 stripping from diethanolamine solution, J. Membr. Sci. 392–393 (2012) 29–37.
[23] A. Mansourizadeh, A.F. Ismail, Effect of additives on the structure and performance of polysulfone hollow fiber membranes for CO_2 absorption, J. Membr. Sci. 348 (2010) 260–267.
[24] A. Mansourizadeh, Experimental study of CO_2 absorption/stripping via PVDF hollow fiber membrane contactor, Chem. Eng. Res. Des. 90 (2012) 555–562.
[25] J.M.S. Henis, M.K. Tripodi, Composite hollow fiber membranes for gas separation: the resistance model approach, J. Membr. Sci. 8 (1981) 233–246.
[26] R.W. Baker, Membrane Technology and Application, John Wiley & Sons Ltd., England, 2004.
[27] M.L. Yewo, Y.T. Liu, K. Li, Isothermal phase diagrams and phase-inversion behavior of poly(vinylidene fluoride)/solvents/additives/water systems, J. Appl. Polym. Sci. 90 (2003) 2150–2155.
[28] Y. Liu, G.H. Koops, H. Strathmann, Characterization of morphology controlled polyethersulfone hollow fiber membranes by the addition of polyethylene glycol to the dope and bore liquid solution, J. Membr. Sci. 223 (2003) 187–199.
[29] D. Singh, K.K. Sirkar, Performance of PVDF flat membranes and hollow fibers in desalination by direct contact membrane distillation at high temperatures, Separ. Purif. Technol. 187 (2017) 264–273.
[30] M. Sadrzadeh, S. Bhattacharjee, Rational design of phase inversion membranes by tailoring thermodynamics and kinetics of casting solution using polymer additives, J. Membr. Sci. 441 (2013) 31–44.
[31] M. Rahbari-sisakht, A.F. Ismail, T. Matsuura, Effect of bore fluid composition on structure and performance of asymmetric polysulfone hollow fiber membrane contactor for CO_2 absorption, Separ. Purif. Technol. 88 (2012) 99–106.
[32] S. Li, H. Zhang, S. Yu, J. Hou, S. Huang, Y. Liu, Pore structure characterization and gas transport property of the penetrating layer in composite membranes, Separ. Purif. Technol. 211 (2019) 252–258.
[33] A.C.M. Franken, J.A.M. Nolten, M.H.V. Mulder, D. Bargeman, C.A. Smolders, Wetting criteria for the applicability of membrane distillation, J. Membr. Sci. 33 (1987) 315–328.
[34] A. Rastegarpanah, H.R. Mortaheb, Surface treatment of polyethersulfone membranes for applying in desalination by direct contact membrane distillation, Desalination 377 (2016) 99–107.
[35] H.J. Hwang, K. He, S. Gray, J. Zhang, I.S. Moon, Direct contact membrane distillation (DCMD): experimental study on the commercial PTFE membrane and modeling, J. Membr. Sci. 371 (1–2) (2011) 90–98.
[36] A. Alkhudhiri, N. Darwish, N. Hilal, Produced water treatment: application of air gap membrane distillation, Desalination 309 (2013) 46–51.
[37] A. Mansourizadeh, A.F. Ismail, M.S. Abdullah, B.C. Ng, Preparation of polyvinylidene fluoride hollow fiber membranes for CO_2 absorption using phase-inversion promoter additives, J. Membr. Sci. 355 (2010) 200–207.
[38] K. Li, J.F. Kong, D. Wang, W.K. Teo, Tailor-made asymmetric PVDF hollow fiber for soluble gas removal, AIChE J. 45 (1999) 1211–1219.